

CHAPTER 5

RESULTS AND DISCUSSIONS

5.1 Effects of transmembrane pressure (TMP) and flow velocity on permeate flux of aqueous extract of *A. ebracteatus* Vahl.

The permeate flux of aqueous extract of *A. ebracteatus* Vahl. through the NF membrane NTR7450 can be calculated based on the experimental data as described in chapter 3. The results are showed in Figure 5.1. We can see that the permeate flux increase with flow velocity at the same applied pressure and generally, at higher transmembrane pressure (TMP), the permeate flux is higher at the same flow velocity. These phenomena have been report by Koyuncu *et al.*, 2003 for wastewater of textile industry containing salt. The increasing of flux with TMP at the same flow velocity can be easily explained by Kedem and Katchalsky equation (Eq. 1) where volume flux is depend on the TMP due to the driving force is pressure difference. These also have been reported for different types of membrane with different solutes (Bowen and Mohammad, 1998; Mohammad *et al.*, 2002; Wang *et al.*, 1995a, 1995b, 2002).

The permeate flux is found to less depend on flow velocity than TMP (Matsubara *et al.*, 1996). However in our study, at flow velocity less than 0.875 m/min, the TMP seems not to effectively increase permeate flux as shown in Figure 5.1 and 5.2. The permeate flux is found to increase from $12.77 \times 10^{-6} \text{ m}^3\text{m}^{-2}\text{s}^{-1}$ to $15.02 \times 10^{-6} \text{ m}^3\text{m}^{-2}\text{s}^{-1}$ when the TMP increases from 10 to 30 kg/cm² at flow velocity of 0.875 m/min. In the same way, at flow velocity of 1 m/min, the permeate flux increases from $14.69 \times 10^{-6} \text{ m}^3\text{m}^{-2}\text{s}^{-1}$ to $20.71 \times 10^{-6} \text{ m}^3\text{m}^{-2}\text{s}^{-1}$ when the TMP increases from 10 to 30 kg/cm². Nevertheless, at flow velocity of 0.75 m/min only slightly increase of permeate flux from $11.64 \times 10^{-6} \text{ m}^3\text{m}^{-2}\text{s}^{-1}$ to $13.29 \times 10^{-6} \text{ m}^3\text{m}^{-2}\text{s}^{-1}$ is observed with the same increase of TMP. These can be explained by the effect of shear rate on concentration polarization and on membrane fouling. The shear rate (γ , s⁻¹) at membrane surface depends on flow velocity as following equation

$$\gamma = \frac{\text{velocity scale}}{\text{length scale}}$$

Thus, higher velocity results in greater shear rate. The increase of shear rate can reduce both of concentration polarization and membrane fouling by the increase

in mass transfer coefficient and the decrease in the concentration on the membrane surface (Bian et al., 2000). Since this system is a system of multicomponents with combination of many different molecular sizes, therefore at low flow velocity might be some large molecules coated or absorbed on the membrane surface or in the pore of membrane causes fouling problem according to low shear rate. Therefore, the increase of TMP at low flow velocity can not improve the permeate flux in this system.

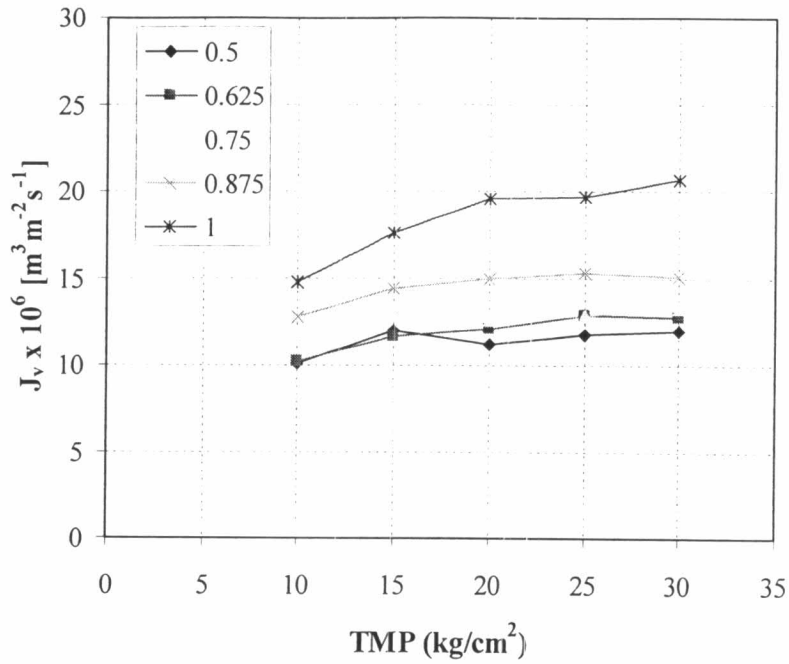


Figure 5.1 Permeate flux of aqueous extract of *A. ebracteatus* Vahl. at different operating conditions. The 0.5; 0.625; 0.75; 0.875 and 1 refer to flow velocities (m/min). The applied pressures varied from 10 to 30 kg/cm².

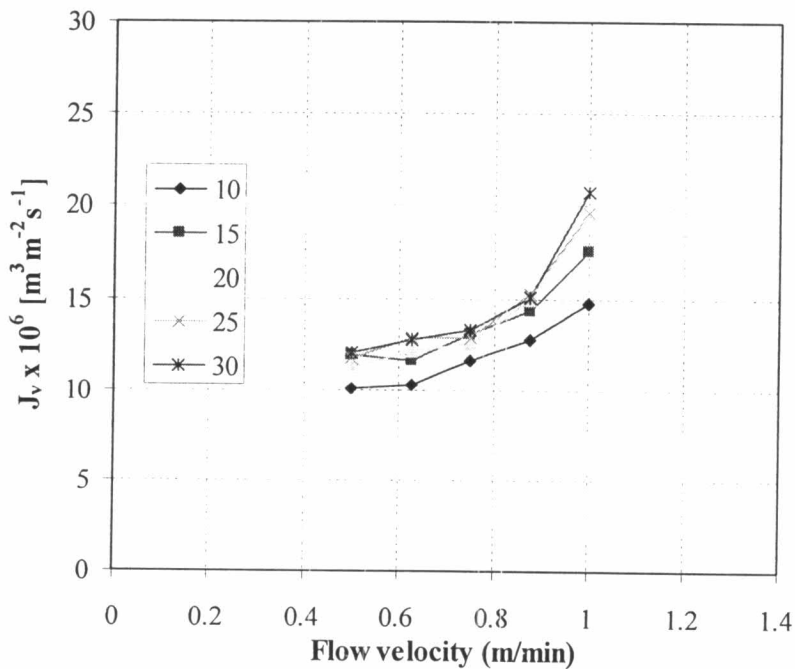


Figure 5.2 Effect of flow velocity on permeate flux of aqueous extract of *A. ebracteatus* Vahl. The 10; 15; 20; 25 and 30 refer to transmembrane pressure (kg/cm²).

5.2 Effect of TMP and flow velocity on observed rejection of sodium chloride

Figure 5.3 shows the effect of flow velocity and TMP on observed rejection rate of sodium chloride. The sodium chloride concentration was measured by AAS.

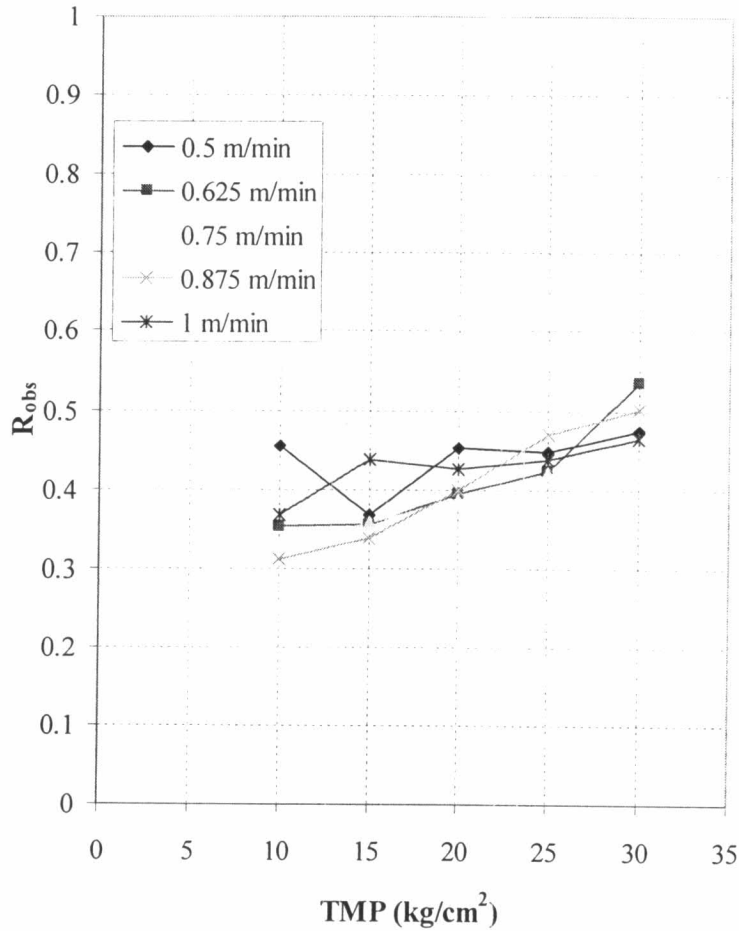


Figure 5.3 NaCl rejection of aqueous extract of *A. ebracteatus* Vahl. at different operating conditions. The experiments were performed at the TMP from 10 kg/cm² to 30 kg/cm² and at flow velocity ranging from 0.5 to 1 m/min.

The rejection of sodium chloride varies from 0.31 to 0.53 and the lowest rejection can be reached at flow velocity of 0.875 l/min and TMP of 10 kg/cm². In general, at the same flow velocity, higher TMP results higher sodium chloride rejection. Similar behavior has been reported for different types of membranes (Ratanatamskul *et al.*, 1998; Wang *et al.*, 2002 and Koyuncu *et al.*, 2003). The reasons have been explained by Wang *et al.*, 2002 that under low operating pressures the solute transport caused by its diffusion is comparable to that accomplished by the convection of the permeation flow through the membranes.

To determine the weight percent of sodium chloride in the total amount of compounds which passed through the membrane, the dry solid of each permeate is measured. The results show that percentage of sodium chloride in permeates varies from 26% to 35% and there were no significant dependency among operating conditions and weight percent of sodium chloride (Table 5.1).

Table 5.1 Weight percent of sodium chloride in dry solid of permeate at different TMP and Flow velocities.

TMP (kg/cm ²)	Flow velocity (m/min)				
	0.5	0.625	0.75	0.825	1
10	30.24	30.96	32.28	33.39	30.70
15	33.30	31.86	31.22	33.18	26.90
20	32.76	32.46	34.00	35.22	27.50
25	34.37	31.46	33.99	30.58	28.69
30	32.68	26.80	34.67	33.62	28.23

5.3 Membrane parameters

For better understanding of the transport phenomena of sodium chloride, the mathematical models are selected as described in chapter 4. The sodium chloride reflection coefficient, σ_{salt} , and solute permeability, P_{salt} , could be determined based on Eq. (3) by fitting curve. In this model, the rejections are found to depend on volume flux as Eq. (3), thus rejection should be dependent on both of flow velocity and TMP as well. The fitting curve is done for each flow velocity and the results are shown in Figure 5.4 and list in Table 5.2. A failed solution occurs at the flow velocity of 0.5 m/min. The negative number of reflection coefficient and solute permeability are obtained for flow rate of 0.625; 0.75 and 0.875 m/min. The model seems to be better agreement with high flow velocity of 1 m/min. At this condition, the reflection coefficient and permeability of sodium chloride are found to be 0.918 and $21.9 \times 10^{-6} \text{ s}^{-1}$, respectively. The results correspond to Wang *et al.*, reported in 1995b and 1997 for single solution of sodium chloride. From these papers, if we calculate the sodium chloride reflection coefficient, σ_{salt} , and solute permeability P_{salt} for solution at the

same sodium chloride concentration based on Steric-Hindrance Pore (SHP) model and Teorell-Meyer-Sievers (TMS) model, the results obtained are $\sigma_{salt} = 0.916$ and $P_{salt} = 32.6 \times 10^{-6} \text{ s}^{-1}$.

Table 5.2 The reflection coefficient, σ_{salt} , and the permeability, P_{salt} of sodium chloride obtained from experiment data by fitting curve. The results then was compared with the report of Wang et al in 1995b and 1997, in their work a single solution containing sodium chloride was used and the experiment was performed at the flow velocity of 1.5 m/min and TMP varying from 30 to 80 kg/cm².

Flow velocity (m/min)	σ_{salt} (-)	P_{salt} (10^{-6} s^{-1})
0.5	Failed	Failed
0.625	-0.084	-5.6
0.75	-0.053	-5.2
0.875	-0.011	-3.5
1	0.918	21.9
From Wang <i>et al.</i> reports in 1995b and 1997	0.916	32.6

The deviations at low flow velocity can be easily explained by fouling effect due to low shear rate. This causes the increase of both of reflection coefficient, σ_{salt} , and the permeability, P_{salt} of sodium chloride from negative numbers to positives with the flow velocity. The reasonable results at the flow velocity of 1 m/min confirm this. One more reason can be cited according to the complexity of feed solution to compare with single solution. This can be confirmed from data of weight percent of sodium chloride in the permeate that not only sodium chloride but also other charge solutes in the aqueous extract of *A. ebracteatus* Vahl. pass through the membrane (as shown in Table 5.5). The reason is more clearly explained by reports of Mohammad *et al.*, 2002 and Wang *et al.*, 2002 that the rejection mechanism depends very much on electrical effect rather than steric effect.

Thus at high flow velocity, the permeation experiment of real system seems to agree with the mathematical models based on Steric-Hindrance Pore (SHP) model and Teorell- Meyer- Sievers (TMS) model due to the reduction of membrane fouling.

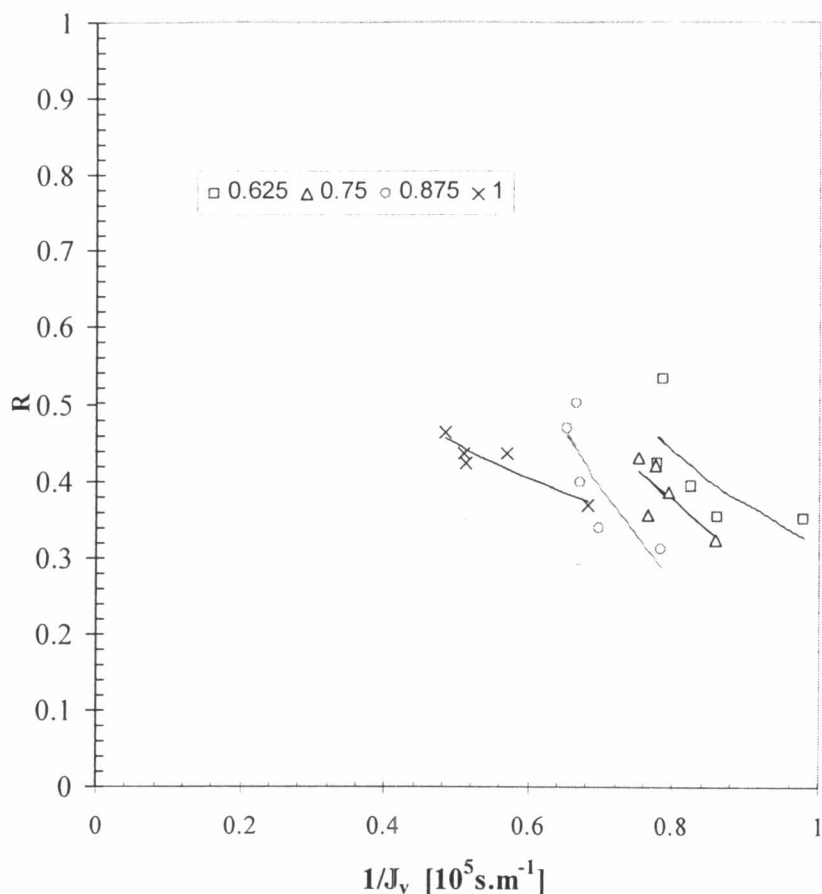


Figure 5.4 Rejection of sodium chloride by NTR7450 membrane as a function of volume flux. The flow velocities were (□) 0.625; (△) 0.75; (○) 0.875 and (x) 1 m/min, respectively. The TMP varied from 10 kg/cm² to 30 kg/cm². The solid lines were fitted by the Spiegler-Kedem equation (Eq. 3) and the dot line is plotted by the Spiegler-Kedem equation with the membrane parameters obtained from the reports of Wang *et al.* in 1995b and 1997. The flow velocity at 0.5 m/min resulted failed solution.

5.4 Optimal conditions consideration

From experimental data we can see that, higher flow velocity and higher TMP result higher flux, but higher TMP results higher sodium chloride rejection as well. Since the objective of this work is to desalinate aqueous extract of *A. ebracteatus* Vahl., so the higher removal of sodium chloride is more important. Thus the operating conditions at which give us the lowest sodium chloride rejection should be considered,

so the optimal conditions are chosen at flow velocity of 0.875 m/min and TMP of 10 kg/cm². Operating at the flow velocity of 1 m/min could reduce fouling effect but the rapidly increasing of feed temperature is observed during experiment with laboratory unit at flow velocity of 1 m/min. This makes difficult to maintain the system.

5.1 Diafiltration process

5.1.1 Concentration step

The second part of NF experiments is performed at flow velocity of 0.875 and TMP of 10 kg/cm². As described before, the diafiltration process has two steps: concentration step and diafiltration step. The concentration factor is 1.5. The permeate flux varying with time and the sodium chloride concentration as function of feed volume are showed in Fig. 5.5 and 5.6. The permeate flux reduces from $9.5 \times 10^{-6} \text{ m}^3 \text{ m}^{-2} \text{ s}^{-1}$ to $6.1 \times 10^{-6} \text{ m}^3 \text{ m}^{-2} \text{ s}^{-1}$ after 14 hours of filtration due to membrane fouling at membrane surface. The experiment data on sodium chloride concentration varying with the feed volume seems to be well agreement with the prediction due to the sodium chloride rejections were quite constant during concentration step (Fig. 5.7).

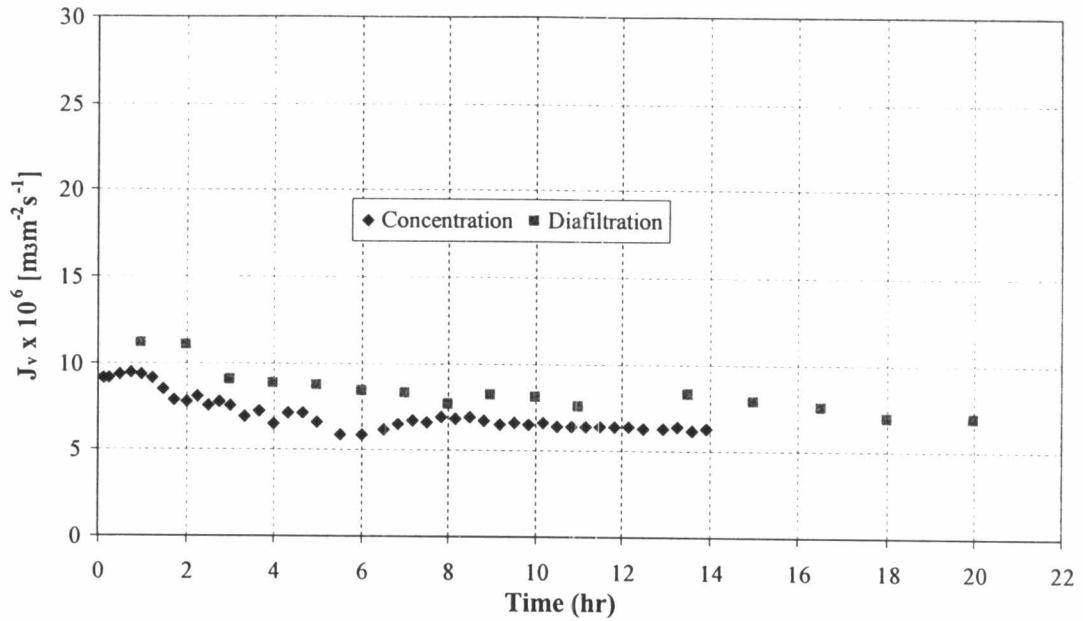


Figure 5.5 Permeate flux at the concentration step and the diafiltration step. The operating conditions are at the TMP of 10 kg/cm^2 and at the flow velocity of 0.875 m/min . The retentate after concentration step was used as initial feed for diafiltration. In diafiltration step, two membrane units were used.

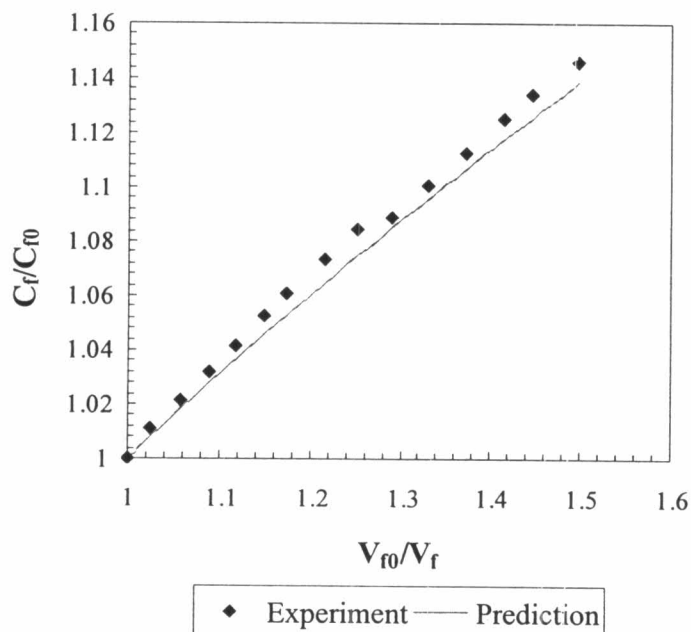


Figure 5.6 C_f/C_0 as a function of V_{f0}/V_f at the concentration step in overall diafiltration process. The prediction curve was plotted by Eq. (22) with the constant sodium chloride rejection of 0.31.

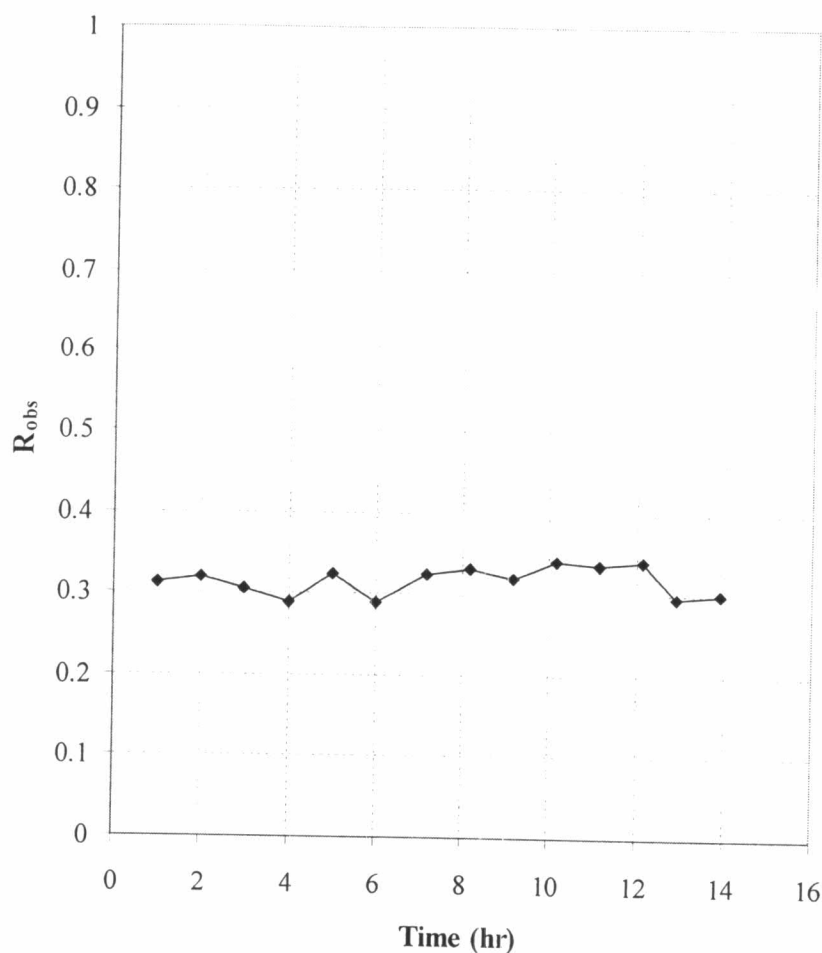


Figure 5.7 Sodium chloride rejection with time at the concentration step. The sodium chloride concentrations were measured by AAS method and the rejections were calculated as described in chapter 3.

5.5.2 Diafiltration step

After the concentration step, the retentate was used as the initial feed for diafiltration step. In diafiltration step, the permeate flux is higher than that of concentration step due to the reducing of the overall solid content in the feed and the reducing of membrane fouling by addition of pure water. This is corresponding to Capelle *et al.* that the diafiltration step is found to limit membrane fouling.

Figure 5.8 shows the concentration of sodium chloride as a function of volume rate of pure water. The calculated data is determined as Eq. (22) with sodium chloride rejection of 0.31. As respected, the experimental data for ratio of feed concentration to

initial concentration are found to correspond to the calculation. By 2 times of diafiltration, the sodium chloride concentration in feed reduces to more than 1/3 and to compare with aqueous extract of *A. ebracteatus* Vahl. The total sodium chloride removal after diafiltration process is about 80% (Table 5.3). According to this model a diafiltration ratio of 3 might be sufficient to remove 90% of sodium chlorides from solution. However, with the limit of filtration area of laboratory NF unit, such a high level of desalinization may not be achieved in acceptable processing time.

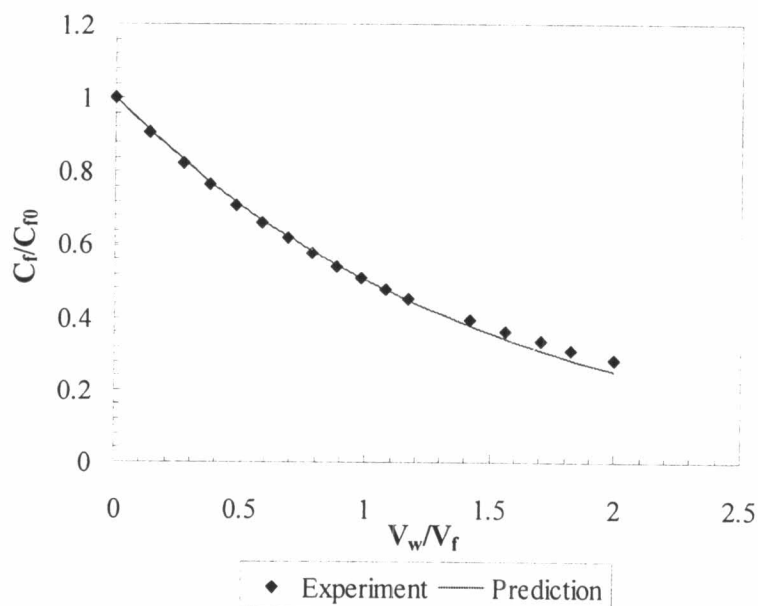


Figure 5.8 Variation of feed concentration during diafiltration step. The prediction curve is plotted by Eq. 24 with the constant sodium chloride rejection of 0.31.

The percentage of sodium chloride in total dry solid of *A. ebracteatus* Vahl. is about 14% w/w, the amount of sodium chloride after concentration and diafiltration step are 11.5% w/w and 5.87% w/w respectively.

Table 5.3 Weight percent of sodium chloride in the total dry solid in initial aqueous extract and retentate after concentration and diafiltration step and the removal of sodium chloride and other compounds than sodium chloride after each step. The experiments were performed at flow velocity of 0.875 m/min and TMP of 10 kg/cm²

Step	Total solid content (g/l)	Weight percent of sodium chloride in dry solid (% w/w)	Removal of sodium chloride (%)	Removal of the other compounds than sodium chloride (%)
Initial aqueous extract	13.6	14	-	-
Retentate after 1.5x Concentration	16.1	11.5	32.3	11.6
Retentate after 2x Diafiltration (concentrate)	9.8	5.87	79.7	36.6

5.6 Percentages of carbon (C), hydrogen (H) and nitrogen (N)

The permeates in all experiment are colorless (Figure 5.9), however, the decrease of total solid content of concentrate is observed and the removals of other compounds free sodium chloride after concentration and diafiltration step are 11.6% and 36.6%, respectively (Table 5.3). Thus it is necessary to determine weight percent of C, H and N in dry solid of initial aqueous extract; retentates and permeate. The data show in Table 5.4. The increase of C and H and the reducing of percentage of N occur for concentrate after diafiltration step. This can be explained by the decreasing of sodium chloride after diafiltration process (with 79.7 % sodium chloride removal). The decrease of N in retentate is possible from small molecules of inorganic source or enzymes with low molecular weight passed through the membrane. The active components in *A. ebracteatus* Vahl. are thought to be polysaccharides, alkaloids and some other macro molecules which could not pass through the membrane. However,

the results on permeate of concentration and diafiltration step show that some organic compounds may also pass through the membrane due to molecular weight cut-off of NF membrane ranges from hundreds to thousands Daltons. These are confirmed by HPLC results (Figure 5.10 to 5.13). Thus it should be important to study on feed properties of aqueous extract of *A. ebracteatus* Vahl. and also the removal of active components should be estimated.

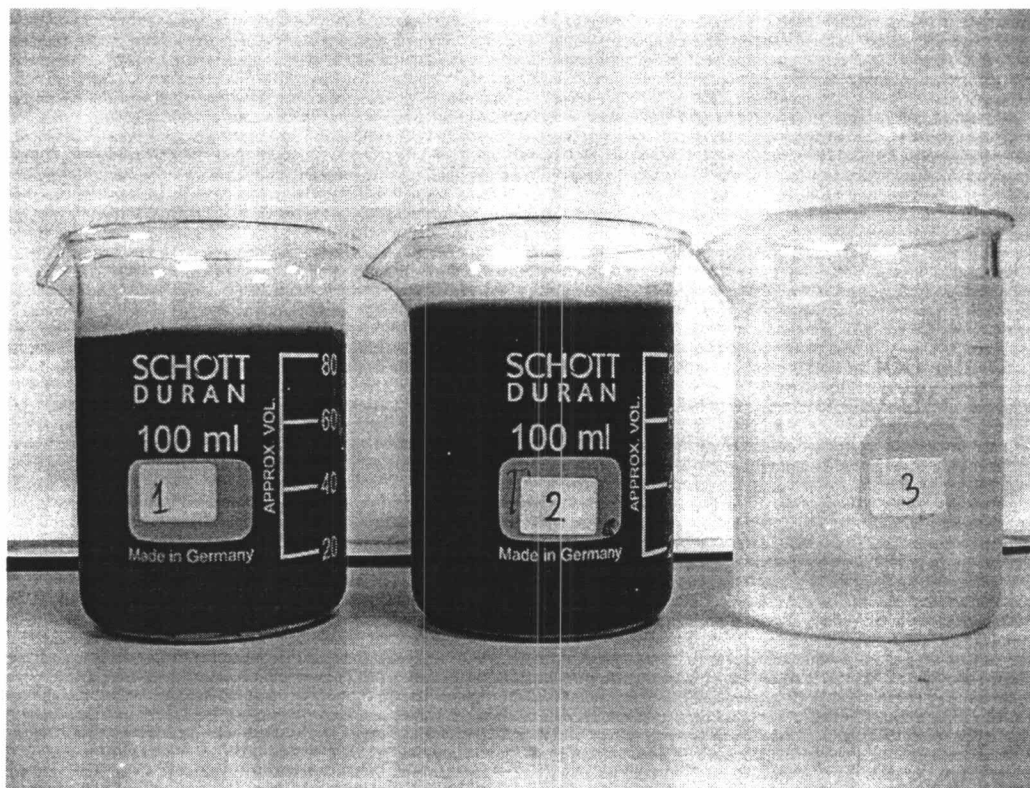


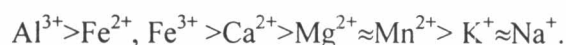
Figure 5.9 The color of initial aqueous extract of *A. ebracteatus* Vahl. (1); concentrate (2) and permeate (3)

Table 5.4 Percentage of NaCl, C, H and N in dry solid of initial aqueous extract, retentate and permeates. The concentrate is the retentate after overall diafiltration process. The experiment was carried out at the optimal conditions.

Step	NaCl (%)	C (%)	H (%)	N (%)
Initial aqueous extract	14	26.824	3.798	0.468
Retentate after 2x Diafiltration (concentrate)	5.87	36.469	4.752	0.348
Permeate at Concentration step	30.5	12.688	2.623	0.364
Permeate at Diafiltration step	35.25	14.017	2.488	0.347

5.7 Removal of other charged solutes

Since the membrane NTR 7450 has negative charge and the rejection mechanism depends very much on electrical effect rather than steric effect (Mohammad *et al.* 2002 and Wang *et al.* 2002), so the higher charge ions should be more selective than monovalent ions. However, the results show that the multivalent ions are retained better than monovalent ions and the order of rejection of cations by NTR7450 membrane is as follows:



This can be explained by report of Wang *et al.* 2002 that the rejection of cations depends on both of charge of cations and the kind of anions. From the paper, the observed rejections to univalent anion electrolytes (NaCl, KCl and MgCl₂) are much smaller than those to bivalent anion electrolytes (Na₂SO₄ and MgSO₄). One more reason can be cited that the observed rejection is also dependent on the concentration. The report of Trusu *et al.* 1991 shows that the rejection of sodium chloride decreases with the concentration.

The rejection order of cations corresponds to the conclusion of Backer W.R. (2000) for reverse osmosis membrane. The similar behaviors have been report by Anne C.O. *et al.*, 2001 for sea water separation by tubular NF membrane from Koch-Weizmann and PCI.

Table 5.5 Concentration and removal of cations in initial aqueous extract, concentrate and permeate at concentration and diafiltration step. The data were obtained by AAS analysis and by calculation based on mass balance. The feed at concentration step was the initial aqueous extract and the retentate after concentration step was used for diafiltration step.

Step Cations	Concentration step				Diafiltration step				Total removal (%)
	Concentration (ppm)			% Removal	Concentration (ppm)			% Removal	
	Feed	Retentate*	Permeate		Feed*	Retentate	Permeate		
Na ⁺	742.17	850.895	524.72	32.30	850.895	226.17	312.3625	73.42	79.70
K ⁺	765	889.125	516.75	22.52	889.125	220.5	334.3125	75.20	80.78
Mg ²⁺	209.5	267.25	94	14.96	267.25	106	80.625	60.34	66.27
Fe ²⁺ , Fe ³⁺	124.5	186.2525	0.995	0.27	186.2525	123.5	31.37625	33.69	33.87
Ca ²⁺	22.6	29.04	9.72	14.34	29.04	16.74	6.15	42.36	50.62
Mn ²⁺	15.375	19.95	6.225	13.50	19.95	7.725	6.1125	61.28	66.50
Al ³⁺	1.66	1.925	1.13	22.69	1.925	1.88	0.0225	3.60	24.50

* The data were calculated based on the mass balance.

5.8 Results of HPLC analysis

Figure 5.10 to 5.13 show the chromatogram of HPLC analysis. After 1.5 concentration step the concentrations of solution were much higher (Fig. 5.11) and the same main peaks but bigger were observed for the retentate compared to these from the initial aqueous extract (Figure 5.10). These may promise the retention of organic compounds after the nanofiltration unit. However, the results of HPLC analysis could not offer enough information to estimate the recovery percentage of organic compound, as well as the identification of bioactive components. The result on permeate shows that at a injection volume of 100 μl (Fig. 5.13a) there were only one main peak at retention of 3.9 min. At the higher the injection volume of 200 μl (Fig. 5.13b), there were some separately peaks at different retention times which are corresponding to the methanol gradient of 10, 20 and 30% volume of methanol in water. These more indicate that some other compounds than salts also passed through the membrane with higher rejection due to the complexity of feed solutions. The presence of carbon in the permeate can be clearly confirmed it.

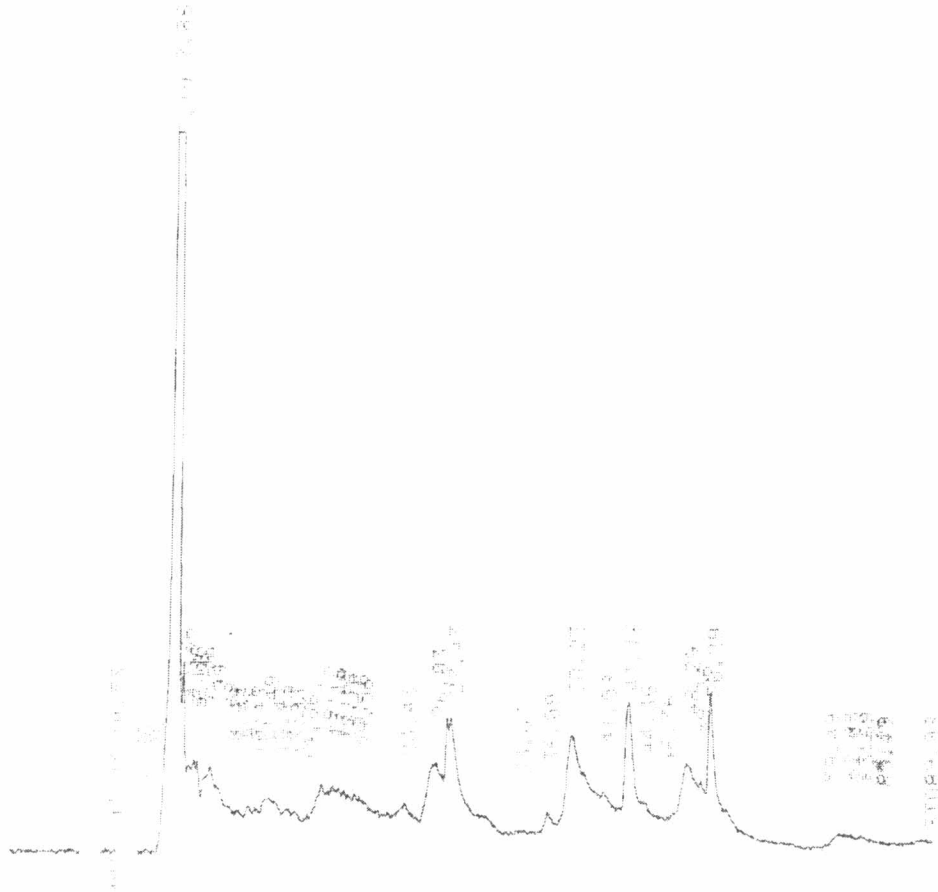


Figure 5.10 The chromatogram of the initial aqueous extract of *A. ebracteatus* Vahl. at injection volume of 100 μ l

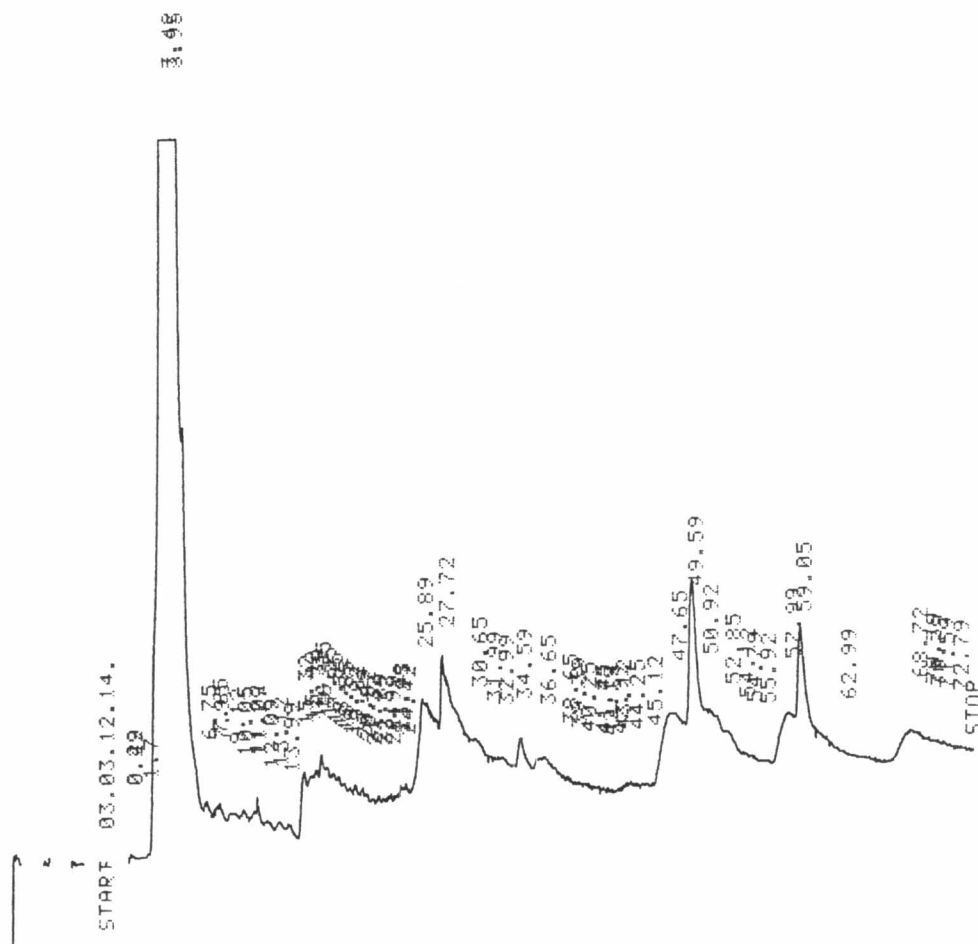


Figure 5.11 The chromatogram of the retentate after concentration step at injection volume of $100 \mu\text{l}$

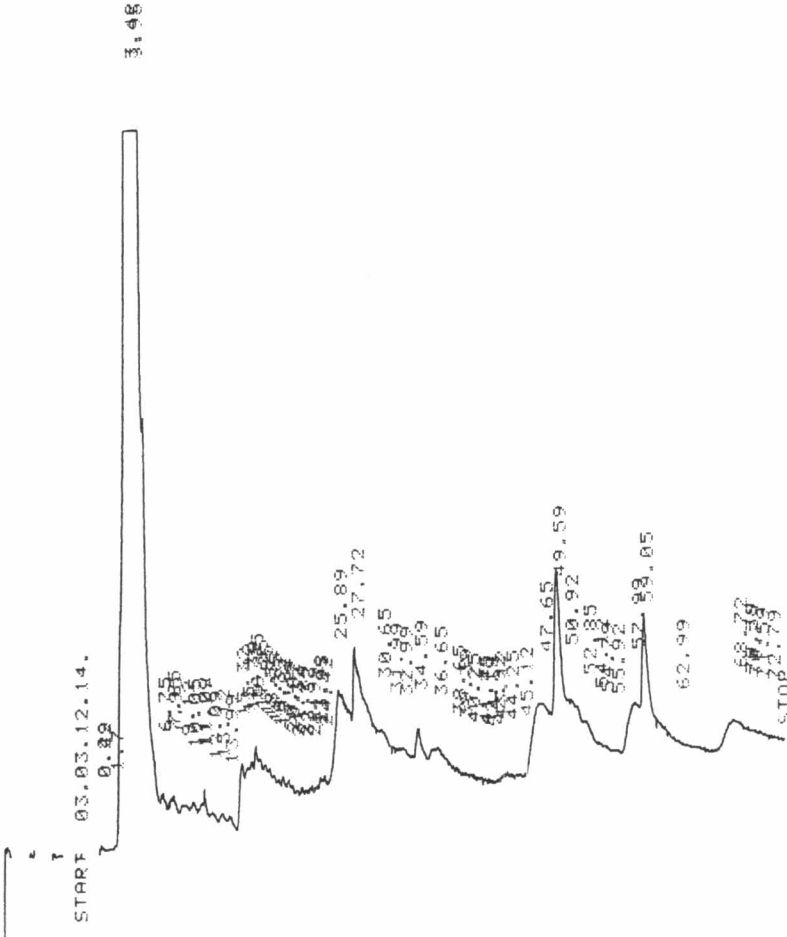


Figure 5.12 The chromatogram of retentate (concentrate) after diafiltration step at injection volume of 100 μl



Figure 5.13a The chromatogram of the average permeate at concentration step at injection volume of 100 μ l.

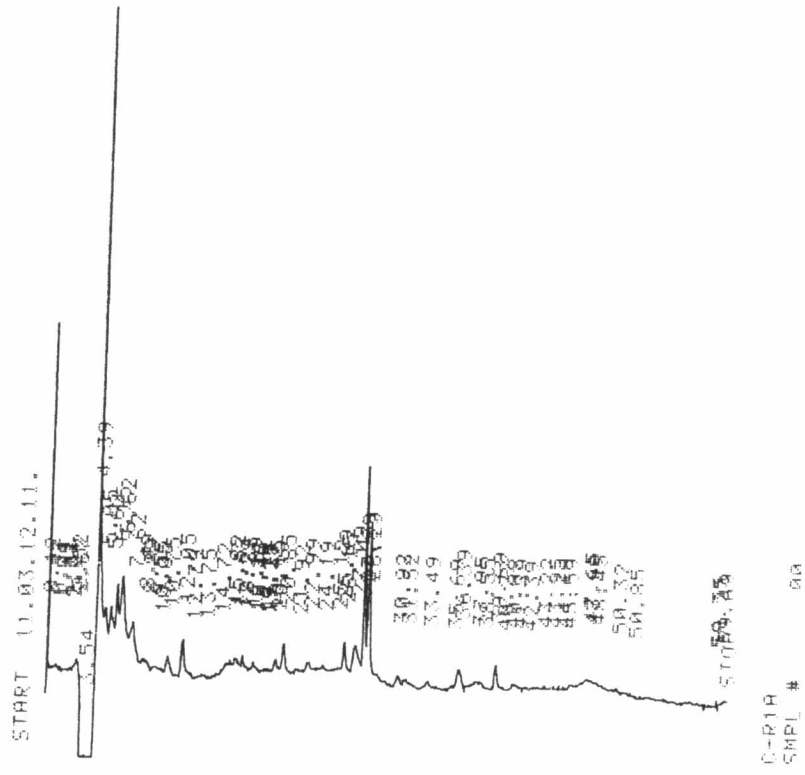


Figure 5.13b The chromatogram of the average permeate at concentration step at injection volume of 200 μ l.

5.9 Bioactivity

The cytotoxic activity of compounds from the initial aqueous extract, the concentrate and the permeate after concentration step and diafiltration step were evaluated against KB (human epidermoid carcinoma) and HeLa (human cervical carcinoma) cell lines employing the MTT colorimetric method (as described in Appendix A). The results of their cytotoxicities are shown in Table 5.6. The concentrate shows the best cytotoxicity against both of KB and HeLa cell lines with IC_{50} values of 3200 and 3500 $\mu\text{g/ml}$, respectively. This explains the low cytotoxicity of initial aqueous extract to compare with the extract after desalinization. Furthermore, the lowest cytotoxic activity of permeates are observed. These may be due to the concentration of bioactive compounds in concentrate is higher compared to the concentration in feed and permeates, respectively. However, very high level of sodium chlorides might also cause the damaged of the cells.

Table 5.6 Cytotoxicity of compounds from the initial aqueous extract, the concentrate and the permeate after the concentration and the diafiltration step. The 50% inhibition concentration IC_{50} was determined by curve fitting as shown in Appendix B and C.

Compounds	Cancer cell lines IC_{50} ($\mu\text{g/ml}$)	
	KB	HeLa
Innitial aqueous extract	4000	3800
Concentrate	3200	3500
Permeate after the concentration step	4800	4200
Permeate after the diafiltration step	5000	4500